Chapter 5

5. Criterion for Factor of Safety of Chain Pillar

5.1 General

This chapter presents the numerical modelling study of the 23 failed and 20 stable cases of pillars in Indian geo-mining conditions. The cover depth of these workings varied from 23 – 450 m, while the w/h ratio of the pillars ranged from 0.57 to 8.3. The modelling approach considered the strain-softening behaviour of the coal pillars, considering degradation of the post-failure strength parameters with the evolution of plastic damage in the coal. The statistical models (Equations 4.1-4.2), developed and validated in the previous chapter, were utilized for estimating the post-failure strength parameters.

The load on the pillar was estimated using the Tributary Area Theory (TAT), except for pillars belonging to Jitpur Colliery shaft area. The load on the shaft pillars was compiled from the Finite Element modelling results reported by Sheorey et al. (1982b). The failure and stress distribution mechanism in the typical pillars were verified by comparing the modelling results with earlier studies. The median value of the factor of safety of the failed pillar cases was adopted as the design criterion for the optimum chain pillar design.

5.2 Failed and Stable Pillar Cases

Tables 5.1-5.2 summarise the failed and stable cases of pillars along with their properties as reported by Sheorey et al. (1987). The depth of the coal seam in the case of the stable pillars varied from 23 to 450 m, while the w/h of the pillar varied from 0.57 to 8.3. The height of the pillar varied from 1.8 to 8.4 m, and the compressive strength of cubical coal samples of 25 mm

edge length varied between 19 and 50 MPa. The in-situ coal strength varied between 3.0 MPa and 16.5 MPa. The database contains only one stable case with w/h greater than 8 (w/h=8.3). Except for the Jitpur pillars, all the failed cases had w/h ≤ 3. Failed and stable pillar cases from the Jitpur shaft area had w/h ratios ranging from 3.08 to 6.67 and 6.4 to 7.6, respectively. All the instances of the failed pillars experienced a controlled failure in the field.

Table 5.1 Collated data of failed pillar cases

S.No.	Mine (seam)	H (m)	h (m)	w (m)	B (m)	w/h	k (MPa)	σ_c (MPa)
1.	Amritnagar (Nega Jamehari)	30	4.5	3.6	5.7	0.8	16.5	45
2.	Amritnagar (Nega Jamehari)	30	6.0	3.6	5.4	0.6	16.5	45
3.	Begonia (Begonia)	36	3.0	3.9	6.0	1.3	7.6	26
4.	Amlai (Burhar)	30	5.4	4.5	4.5	0.83	5.9	25
5.	Sendra Bansjora (X)	23	8.1	4.65	5.55	0.57	6.7	24
6.	W. Chirimiri (Main)	90	3.75	5.4	6.0	1.44	11.2	45
7.	Birsingpur (Johilla top)	129	3.6	7.5	6.0	2.08	8.8	38
8.	Pure Kajora (Lower Kajora)	54	3.6	5.4	6.0	1.5	7.2	33
9.	Pure Kajora (Lower Kajora)	56	3.6	4.95	6.45	1.38	7.2	33
10.	Shankarpur (Jambad bottom)	42	4.8	4.5	4.5	0.94	10.6	47
11.	Ramnagar (Begunia)	70	1.8	2.85	3.15	1.58	7.6	26
12.	Ramnagar (Begunia)	51	1.8	3.0	3.6	1.67	7.6	26
13.	Kankanee (XIII)	160	6.6	19.8	4.2	3.0	4.4	27
14.	Kankanee (XIV)	140	8.4	18.6	5.4	2.2	5.7	25
15.	Jitpur (XIV)	450	3.6	18×34.5	6	6.5	3.0	19
16.	Jitpur (XIV)	450	3.6	10.5×12	6	3.08	3.0	19
17.	Jitpur (XIV)	450	3.6	12×21	6	4.13	3.0	19
18.	Jitpur (XIV)	450	3.6	18×21	6	5.33	3.0	19
19.	Jitpur (XIV)	450	3.6	18×25.5	6	5.83	3.0	19
20.	Jitpur (XIV)	450	3.6	15×63	6	6.67	3.0	19
21.	Jitpur (XIV)	450	3.6	18×30	6	6.25	3.0	19
22.	Jitpur (XIV)	450	3.6	18×30	6	6.25	3.0	19
23.	Jitpur (XIV)	450	3.6	30×43.5	6	5.67	3.0	19

Table 5.2 Collated data of stable pillar cases

S.No.	Mine (seam)	H (m)	h (m)	w (m)	B (m)	w/h	k (MPa)	σ_c (MPa)
1.	Belampalli (Ross)	36	3.0	5.4	6.0	1.8	12.4	48
2.	Nimcha (Ninga)	48	6.0	9.9	6.0	1.7	11.8	50
3.	Morganpit (Salarjung)	270	3.0	8.1	3.6	2.7	11.4	46
4.	Ramnagar (Ramnagar)	75	2.7	9.9	6.6	3.7	6.2	28
5.	Lacchipur (Lower Kajora)	38	5.1	7.2	3.9	1.4	7.2	33
6.	N. Salanpur (X)	30	5.1	9.0	6.0	1.8	5.8	21
7.	Bankola (Jambad top)	102	4.8	10.1	2.4	2.1	11.9	35
8.	Bankola (Jambad top)	75	3.0	6.3	4.2	2.1	11.4	35
9.	Surakacchar (G-1)	106	3.5	16.0	4.0	4.6	13.2	29
10.	Lacchipur (Lower Kajora)	38	5.1	18.3	4.2	3.6	7.2	33
11.	Sripur (Koithee)	266	4.8	40.0	5.0	8.3	6.1	43
12.	E. Angarpathra (XII)	30	2.1	6.0	6.0	2.9	7.0	19
13.	Kargali Incline (Kathara)	36	3.6	9.3	5.7	2.6	8.1	40
14.	Jamadoba 6 & 7 Pits (XVI)	80	2.0	5.8	5.5	2.9	6.8	29
15.	Topsi (Singharan)	85	1.8	7.0	3.9	3.9	11.0	41
16.	Jitpur (XIV)	450	3.6	21×39	6	7.6	3.0	19
17.	Jitpur (XIV)	450	3.6	18×48	6	7.3	3.0	19
18.	Jitpur (XIV)	450	3.6	19.5×30	6	6.5	3.0	19
19.	Jitpur (XIV)	450	3.6	18×31.5	6	6.4	3.0	19
20.	Jitpur (XIV)	450	3.6	15×42	6	7.0	3.0	19

In the above Tables, H, h, w, and B cover depth, pillar height, pillar width, and bord width, respectively. k is the in-situ strength of the coal seam, and $\boldsymbol{\sigma_c}$ is the intact rock compressive strength.

The shaft pillar area of Jitpur Colliery was approximately 240 m × 240 m. Two longwall panels were worked out with hydraulic stowing in three lifts, and one panel was worked in a single lift around this area. The physical evidence of severe spalling, high convergence rate and roof falls in the nearby area indicated that the pillars had been crushed, which was further confirmed by the borehole extensometer observations (Sheorey et al., 1982b).

5.3 Estimation of Rock Mass Properties of Coal

Numerical modelling involving strain-softening constitutive behaviour requires several elasticity and strength parameters of the rock mass. Since many of the properties of the failed and stable pillar cases were not known, the numerical modelling under the limited data

condition necessitated certain assumptions. Since the coal pillar is the weakest link in a system where the roof and floor strata are composed of sandstone, the failure was assumed to occur through pillars. Accordingly, the roof and floor strata were assigned an elastic constitutive model. A similar approach was also used by Badr (2004) and Oraee et al. (2010) to study the stability of pillars.

The elastic modulus of the roof and floor rock and the coal were assumed to be 7 and 2 GPa, respectively, and the Poisson's ratio was uniformly taken as 0.25. The friction angle and cohesion of coal were estimated using the Sheorey failure criterion for the rock mass (Sheorey, 1997) as detailed in Section 3.5, Chapter 3. Since the core samples and their detailed geo-mechanical data were not available, the Bieniawski (1976) RMR were estimated based on certain assumptions. The RQD was treated as proportional to the in-situ strength of the coal seam, considering that the strength is influenced by the presence of joints. The joint spacing of 50-300 mm was considered for all the coal seams.

Similarly, the joints were considered to have a separation of less than 1 mm with slightly rough surfaces and soft wall rock. A dry groundwater condition existed in all the cases (Sheorey et al., 1986). Figure 5.1 shows the bar chart of the estimated RMR for different coal seams. The W-D model (Section 3.4.2, Chapter 3) was employed to model the dilatancy of coal pillars wherein the dilation angle is mobilized as the function of inelastic strain and confining stress.

Figure 5.1 Estimated values of RMR76 for all pillar cases

5.4 Numerical Modelling of the Pillar

A quarter of the pillar geometry was modelled considering the symmetry conditions to simulate the failed and stable pillar cases (Figure 3.9). The uniform zone size of 0.5m × 0.5m× 0.5m was kept in the coal pillar. The fine and uniform size of the brick-shaped zone in the pillar was increased gradually, moving away from it to optimize the computational time and modelling accuracy. The details of the formulation and modelling scheme have been presented in Section 3.11, Chapter 3. The in-situ stresses were initialized in the model using elasto-static thermal stress model proposed by Sheorey (1994).

The properties of interfaces between pillar-roof and pillar-floor were estimated to be 0.18 MPa and 24^{o}, respectively, based on laboratory tests on Indian rocks (Das et al., 2019). The MCSS material model was assigned to the pillar to study its behaviour for the complete range of deformation. The post-peak degradation of strength parameters in the constitutive model was estimated using the set of statistical relations in Equations 4.1-4.4 (Section 4.5, Chapter 4).

5.5 Modelling Results

The vertical stress and strain in all the zones of the pillar were continuously monitored and recorded using FISH routines. The average stress and strain induced in the pillar were calculated as the average of all the zones. The pillar strength was obtained from the stress-strain curve as the peak strength of the pillar. The pillar load was determined using Tributary Area Theory (TAT) (Equation 5.1). The load on the shaft pillars of the Jitpur Colliery was compiled from the Finite Element modelling results reported by Sheorey et al. (1982b), as these pillars were subjected to additional load due to the extraction of workings around them. Tables 5.3 - 5.4 show the safety factor of all the failed and stable pillars, along with their pillar load and strength.

$$\text{Pillar load} = 0.025\text{H}\frac{(\text{w}+\text{B})^2}{\text{w}^2} \tag{5.1}$$

where, pillar load is in MPa and w, B, and H are pillar width, bord width, and the cover depth of the pillar.

Table 5.3 Pillar load and strength of failed pillars along with their factor of safety

S.No.	Mine (seam)	Pillar load (MPa)	Pillar strength (MPa)	FoS
1.	Amritnagar (Nega Jamehari)	5.01	4.43	0.88
2.	Amritnagar (Nega Jamehari)	4.69	3.6	0.77
3.	Begonia (Begonia)	5.8	3.9	0.67
4.	Amlai (Burhar)	3	2.19	0.73
5.	Sendra Bansjora (X)	2.77	1.8	0.65
6.	W. Chirimiri (Main)	10.03	8.03	0.8
7.	Birsingpur (Johilla top)	10.45	8	0.77
8.	Pure Kajora (Lower Kajora)	6.02	5.32	0.88
9.	Pure Kajora (Lower Kajora)	7.43	5.5	0.74
10.	Shankarpur (Jambad bottom)	4.2	5.05	1.2
11.	Ramnagar (Begunia)	7.76	5.44	0.7
12.	Ramnagar (Begunia)	6.17	5.63	0.91
13.	Kankanee (XIII)	5.88	6.5	1.11
14.	Kankanee (XIV)	5.83	5.75	0.99
15.	Jitpur (XIV)	17.75	15	0.85

16.	Jitpur (XIV)	16.23	10.4	0.64
17.	Jitpur (XIV)	17.82	11	0.62
18.	Jitpur (XIV)	16.16	13.3	0.82
19.	Jitpur (XIV)	17.13	14.2	0.83
20.	Jitpur (XIV)	20.51	14.4	0.7
21.	Jitpur (XIV)	18.23	14.7	0.81
22.	Jitpur (XIV)	17.13	14.7	0.86
23.	Jitpur (XIV)	15.81	13.2	0.83

Table 5.4 Pillar load and strength of stable pillars along with their factor of safety

S.No.	Mine (seam)	Pillar load (MPa)	Pillar strength (MPa)	FoS
1.	Belampalli (Ross)	4.01	10.4	2.59
2.	Nimcha (Nega)	3.1	8.8	2.84
3.	Morganpit (Salarjung)	14.08	13.72	0.97
4.	Ramnagar (Ramnagar)	5.21	11.4	2.19
5.	Lacchipur (Lower Kajora)	2.26	4.77	2.11
6.	N. Salanpur (X)	2.08	3.83	1.84
7.	Bankola (Jambad top)	3.91	8.76	2.24
8.	Bankola (Jambad top)	5.21	9.46	1.82
9.	Surakacchar (G-1)	4.14	16	3.86
10.	Lacchipur (Lower Kajora)	1.44	11.6	8.06
11.	Sripur (Koithee)	8.42	34.56	4.1
12.	E. Angarpathra (XII)	3	6.91	2.3
13.	Kargali Incline (Kathara)	2.34	9.92	4.24
14.	Jamadoba 6 & 7 Pits (XVI)	7.59	10.6	1.4
15.	Topsi (Singharan)	5.15	18.2	3.53
16.	Jitpur (XIV)	15.33	16	1.04
17.	Jitpur (XIV)	15.81	15.9	1.01
18.	Jitpur (XIV)	16.64	15.2	0.91
19.	Jitpur (XIV)	14.92	15	1.01
20.	Jitpur (XIV)	15.68	15.7	1.00

Figure 5.2 illustrates the strength vs load plot of failed pillars (plotted in red triangular marker) and stable pillars (shown in green square marker). The diagonal line represents the condition where pillar load is equal to the pillar stress. It can be seen that, except in a few cases, most of the failed pillar cases have a factor of safety less than '1', and most of the stable pillar cases have a factor of safety greater than '1' (Fig. 5.3). Hence, the modelling approach adopted in

this work can distinguish failed and stable pillars quite successfully, except for the failed pillar at Shankarpur (Jambad bottom) and Kankanee (XIII) coal seams and the stable pillar of Morganpit (Salarjung) and Case 18 of Jitpur (XIV) coal seam. The median value of the safety factor of the failed pillar cases, excluding the exceptional cases, was 0.78.

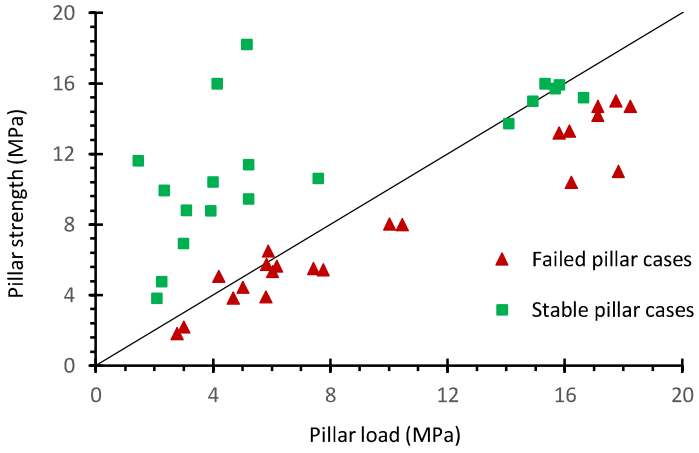

Figure 5.2 Model strength versus pillar load of the failed and stable pillar cases from Table 5.3 and 5.4

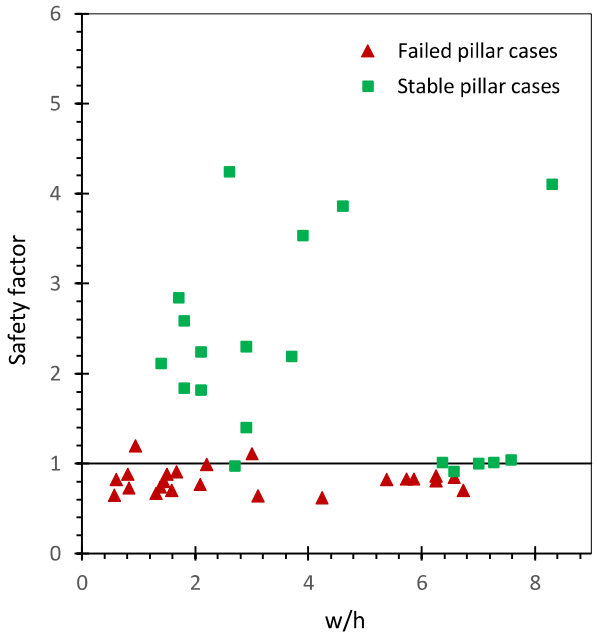

Figure 5.3 Factor of safety of the failed and stable pillars, the horizontal line at the safety factor of '1' separates most of the failed and stable pillars quite successfully

The stress-strain characteristics of the coal pillars for w/h ratio of 0.6 (Case 2, failed pillars), 3.6 (Case 10, stable cases), and 6.35 (Case 21, failed cases) are shown in Figure 5.4. The starting ordinate value of the stress-strain curve corresponds to the cover pressure. It is seen that the non-zero confining stress (σ_3) in the pillar is more for a higher w/h ratio at this stage. As the axial strain continues, the pillar stress increases to attain peak strength. Thereafter, it decreases gradually till the residual strength. However, for the pillar of w/h equal to 6.35, the axial stress curve rises again after the residual strength due to the confinement provided by the reconsolidated failed coal material, as reflected by a gradual increase in the confining stress beyond the residual strength. For the w/h ratio of 3.6, the residual strength remains maintained

for the complete range of axial strain, but the pillar having a w/h of 0.6 exhibits zero residual strength. The confining stress for the latter is almost negligible, whereas it is substantial in the former case. These findings corroborate well with the modelling results of coal samples of various w/h ratios described in Chapter 4 and laboratory test results reported by Das (1986). These outcomes also validate the modelling procedure and the statistical model for post-peak strength parameters.

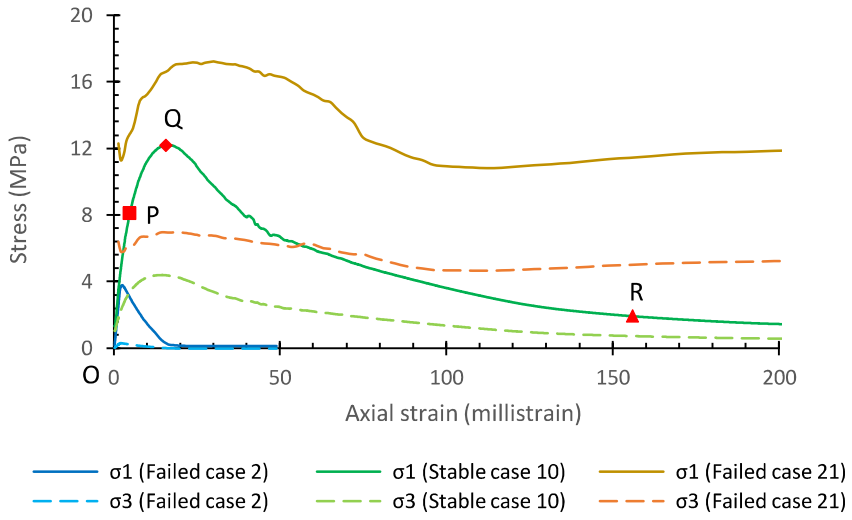

Figure 5.4 Stress-strain behaviour of pillars for the failed cases 2 and 21 and the stable case 10

Fig. 5.5 shows the distribution of (a) failure, (b) vertical stress in the pillar, and (c) interface shear slip and displacement for a typical coal pillar of 18.3m×18.3m size (stable pillar, case 10) at two-third of the peak strength (point P), peak strength (point Q), and residual strength (point R) (Please refer the square, rhombus and triangle-shaped marker in Fig. 5.4). For better visualization, the failure and stress distribution are shown separately for the upper (inverted) and the lower halves of the pillar.

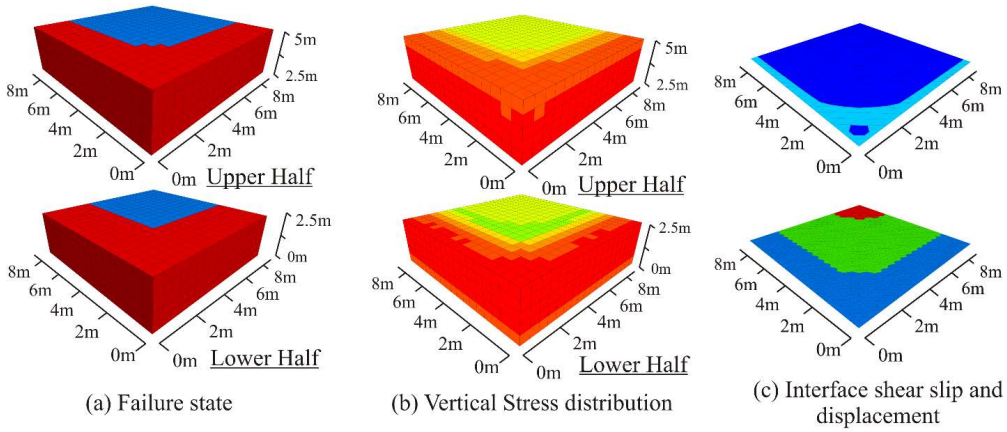

(p) Two-third of the peak strength

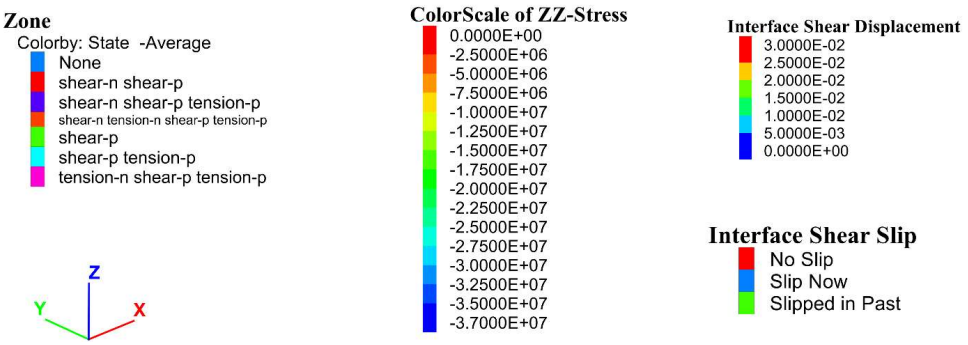

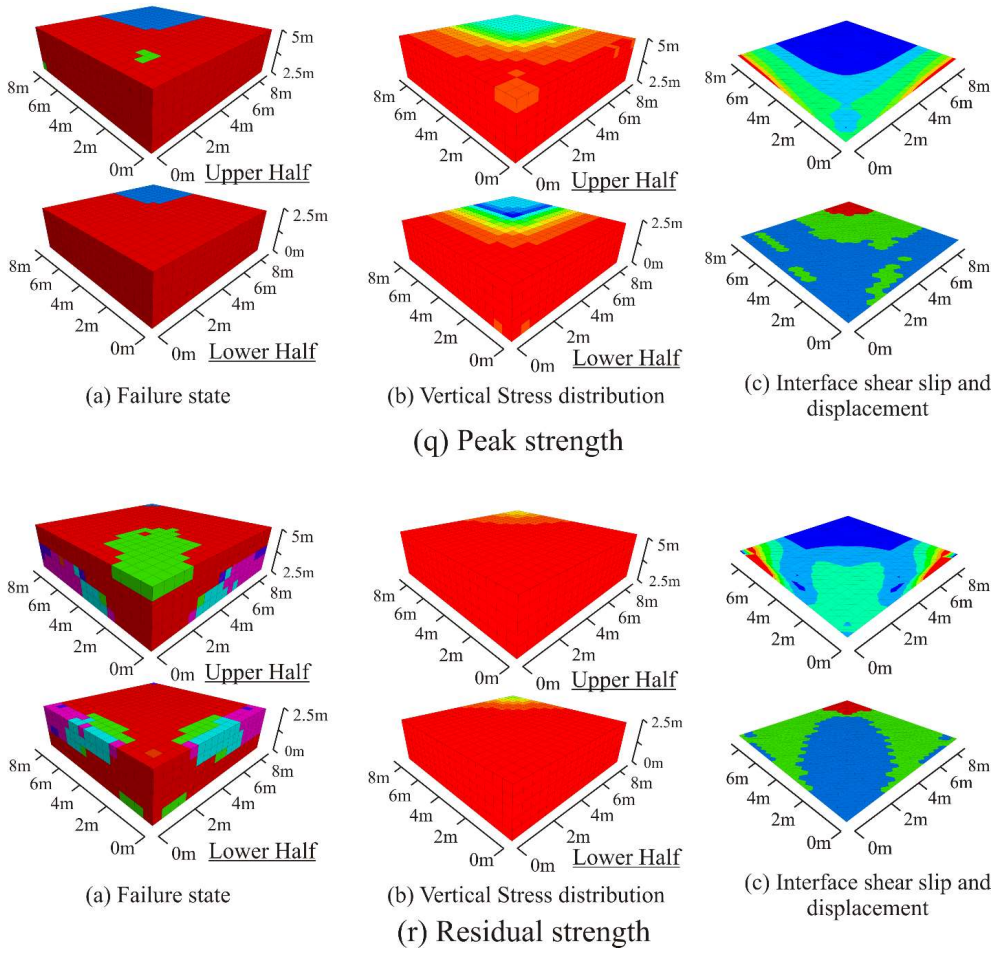

Figure 5.5. Pattern of (a) failure, (b) Vertical stress, (c) interface shear slip and displacement at upper and lower halves of the pillar at (p) two-third of peak strength, (q) peak strength, and (r) residual strength of stable pillar case 10. (Points P, Q and R are marked as square, rhombus and triangle markers in Figure 5.4).

It is observed that the pillar behaves elastically in the region O-A and begins to yield after that (Figure 5.4). At point A, the sides of the pillar have yielded, but a substantial core is in the elastic state (Figure 5.5(p)(a). The yield zone penetrated slightly deeper at the middle level compared to the upper portion. Therefore, the maximum vertical stress concentration of 14MPa is located relatively deeper in the core at the middle level than the vertical stress concentration of approximately 10MPa at the top level of the pillar. The yielding is accompanied by slippage

of the interface. The slippage of the interface occurred around the rib area, whereas 'no slip' is observed above the core area of the pillar (Figure 5.5 (p)(c)). The 'slipped in the past' state of the interface is due to the transient stresses during the initial solution steps of the model and is regarded as a 'no slip' state during the analysis. The plot of interface shear displacement also confirmed that the relative displacement took only around the rib area of the pillar.

In the region P-Q, the pillar showed strain-hardening characteristics as the percentage of the yield zone is significantly lower than the elastic core. At point Q, the pillar achieved its maximum strength. At this point, the pillar achieved substantial yielding towards the core, and only a small elastic core was present (Figure 5.5 (b)). The yielding occurred relatively deeper towards the core at the middle level than at the top level of the pillar. The maximum vertical stress concentration of around 35MPa was observed at the middle level of the core in comparison to 28MPa at the top level of the pillar. A similar trend was observed for the shear slip and displacement of the interface.

In the region Q-R, the pillar showed the strain-softening behaviour as the smaller elastic core which was carrying the load in the previous stage, also began to yield. At point R, the pillar attained the residual strength upon yielding of the entire core (Figure 5.5 (r)(a)). The core at the middle and the top of the pillar yielded completely. As a result, the maximum concentration of vertical stress at the pillar centre was reduced to 12MPa at the middle and 7 MPa at the top level of the pillar. The slip state combined with the shear displacement of the interface showed that the slip occurred almost up to the core, barring only a small portion of the pillar core that showed the 'no slip' state. The pillar maintained some residual strength because of the combined effect of the confinement provided by the yielded material and the 'no slip' zone around the core.

5.6 Design Criterion

All the cases of failed pillars considered in this study had received a controlled failure, especially pillars with a greater w/h ratio. Further, none of the pillars with a w/h ratio greater than 3 was reported to fail suddenly. The failed pillar of the Jitpur Colliery shaft area had squeezed to failure with side slabbing and some extent of rook fall, as evident from the field observations. These failed pillars had w/h of 3.08 to 6.67.

Chain pillars are designed with the functional objective of providing physical isolation between the adjacent longwall panels. Hence, the pillars are required to remain stable till both the adjacent panels are mined-out. After the extraction of both the adjoining panels, they are supposed to fail to produce a smooth subsidence profile at the surface. The design criterion for stability of the chain pillar is based on this premise in the present work. Accordingly, the median factor of safety of 0.78 for the set of the failed pillars is proposed as the criterion for the design of chain pillars in this work.

5.7 Summary

A numerical modelling study was conducted to simulate the behaviour of 23 failed and 20 stable pillars cases in Indian geo-mining conditions. The cover depth and the w/h ratio of these pillars varied from 23-450 m and 0.57-8.3, respectively. The strength of the pillar was obtained from the peak value of the stress-strain curve, while the pillar load was estimated using the Tributary Area Theory (TAT). The load on the shaft pillars of the Jitpur Colliery was compiled from the Finite Element modelling results reported by Sheorey et al. (1982b). The statistical model developed in Section 4.5, Chapter 4, was used to model the strain-softening behaviour of the coal pillars. The W-D dilation model was employed to simulate the mobilization of the dilation angle with the plastic shear strain. Since the failure was primarily limited to the coal

pillar, the elastic constitutive model was assigned to roof and pillar strata, and the contact surfaces between the roof-pillar and floor-pillar were modelled using interface elements.

The modelling approach was able to simulate failed and stable pillars, as most of the failed pillars showed a factor of safety less than 1, whereas stable pillars had FoS greater than 1. Further analysis of the modelling outcomes in terms of stress-strain characteristics of the pillars showed that the pillars exhibit different post-failure behaviour, from brittle to softening with an increase in the w/h ratio. For a high w/h ratio (w/h = 6.35), the model showed regain in strength after achieving the residual strength beyond the initial phase of softening. These observations are in line with the laboratory testing-based findings of Das (1986).

The plots of failure state, vertical stress contour, and shear slip along the interface of the pillar showed that the failure in the pillar having w/h of 3.6 progressed from the sides towards the core with the increase in the axial strain. The failure at the middle of the pillar was deeper in comparison to the failure at the roof and floor level due to the shear resistance offered by the contact surfaces. While the pillar retained a small elastic core at its peak strength, the entire core failed when the residual strength was attained. The residual strength was primarily due to the confining effect of the failed coal around the core and the contact surfaces at the ends.

The aspect of controlled failure in the failed pillars was utilized to develop the criterion for chain pillar design. Considering that the chain pillars, mainly designed to provide physical isolation between the adjacent longwall panels, should fail as soon as both the adjoining panels are extracted, the median FoS of 0.78 of the set of failed pillars was used as the design limit of the FoS.